Free Radicals in an Adamantane Matrix. 13. Electron Paramagnetic Resonance Study of σ^*–π^* Orbital Crossover in Fluorinated Pyridine Anions

Moon B. Yim, Silvio DiGregorio, and David E. Wood*

Contribution from the Department of Chemistry, University of Connecticut, Storrs, Connecticut 06268. *Received October 18, 1976*

Abstract: Pentafluoropyridine, 2,3,4,6-tetrafluoropyridine, 2,6-difluoropyridine, and 2-fluoropyridine anion radicals were produced by x irradiation of an adamantane matrix which was doubly doped with the aromatic precursors and Me_3NBH_3 and their EPR spectra obtained. The large fluorine hyperfine splitting constants (hfsc) of penta- and 2,3,4,6-tetrafluoropyridine anions and the small fluorine hfsc's of 2,6-di- and 2-fluoropyridine anions suggest that the former two are σ radicals while the latter two are π radicals. The σ^*–π^* orbital crossover phenomenon observed in these fluorinated pyridine anions is explained in terms of the *combined* effects of stabilization of σ^* orbitals and destabilization of π^* orbitals. The EPR results show that nitrogen has a negligible contribution to the unpaired electron σ^* orbitals. INDO calculations were performed for the various states and the results compared with experiment.

I. Introduction

The comparison of electron paramagnetic resonance (EPR) spectra of fluorinated radicals with that of their hydrogen-substituted counterparts has attracted considerable interest[1-6] since this, in principle, allows measurement of the effect of fluorine substitution on molecular orbitals and the concomitant changes in geometry and electronic structure of the radicals. We have reported EPR studies of the systematic substitution of fluorine in cyclohexadienyl[2] and benzene anion[3] radicals, and in some alkyl radicals.[4] These results have shown that fluorine substitution moderately affects energy levels of the cyclohexadienyl and perfluoroalkyl radicals such that the effective hyperconjugation is reduced for β-fluorine and thus the β hyperfine splitting constants (hfsc) are also reduced. More dramatic effects have been found in the fluorinated benzene anion series; the lightly fluorinated benzene anions are π radicals, while heavily fluorinated benzene anions are σ radicals. The σ^*–π^* orbital crossover phenomenon in the fluorinated benzene anion series is unique and similar effects were sought in the fluorinated pyridine series.

We present here an EPR study of radical anions of pentafluoropyridine, 2,3,4,6-tetrafluoropyridine, 2,6-difluoropyridine, and 2-fluoropyridine prepared by x irradiation of an adamantane matrix doubly doped with trimethylamineborane (Me_3NBH_3) and the anion precursors.

II. Experimental Section

The following chemicals were used as received: (1) 2-fluoropyridine (K&K Laboratories, Inc., Plainview, N.Y.); (2) 2,6-difluoropyridine; (3) pentafluoropyridine; (4) trimethylamineborane (Peninsular Chemical Research Inc., Fla.); (5) 2,3,4,6-tetrafluoropyridine (a gift from Mond division, Imperial Chemical Industries, Ltd. Great Britain). The EPR spectrometer, accessories, and experimental procedures for sample preparation have been described elsewhere.[2-3]

III. Results

A. Pentafluoropyridine Anion. Adamantane doped with pentafluoropyridine and Me_3NBH_3, then x irradiated at 77 K yields the pentafluoropyridine anion radical, whose EPR spectrum at 236 K is shown in Figure 1 together with a computer simulation based on the parameters of Table I: A_N = 3.55, A_2 (2) = 61.2, A_3 (2) = 17.4, A_4 = 249, and line width = 2.10 G. The identity of the intense lines in the center of the spectrum is not known. The lack of good 1:2:1 intensity ratio of the A_2 (2) = 61.2 G splittings results from second-order effects. INDO calculations for the σ radical (vide infra) indicates that $A_2 > A_3$; therefore the parameters were assigned as shown in Table I.

B. 2,3,4,6-Tetrafluoropyridine Anion. The EPR spectrum of 2,3,4,6-tetrafluoropyridine anion radical in an adamantane Me_3NBH_3 matrix at 215 K is shown in Figure 2 together with a computer simulation based on the parameters of Table I: A_N = 6.05, A_2 = 59.4, A_3 = 6.05, A_4 = 226, and A_6 = 24.9 G, with a line width of 2.10 G. The central part of the spectrum decays differently from the rest of the lines and must originate from some other radical species. By the time the sample had been warmed to 260 K, the lines of the anion had almost disappeared; however there were many lines spread on the whole spectrum. These lines match well with the lines originating from x-irradiated neat Me_3NBH_3, which was suggested to result from the Me_2NBH_3 radical by Claxton et al.[7] On the basis of the pentafluoropyridine anion assignment and INDO calculation of the σ radical (vide infra), the parameters were assigned as shown in Table I.

C. 2,6-Difluoropyridine Anion. The second derivative EPR spectrum of 2,6-difluoropyridine anion at 188 K is shown in Figure 3. The spectrum is quite simple and it is well simulated based on the parameters of Table I; A_N = 4.20 and A_4 = 10.20 G with line width = 3.0 G.

D. 2-Fluoropyridine Anion. The EPR spectrum of 2-fluoropyridine anion radical in an adamantane Me_3NBH_3 matrix at 183 K is shown in Figure 4 compared with its computer simulation based on the parameters of Table I with line width = 3.0 G. Buick et al.[8] have reported the EPR spectrum of the 2-fluoropyridine anion obtained by liquid ammonia flow experiments. Their assignments[1,8] of hfsc's agree well with those of the pyridine anion[9] and our INDO result (vide infra). We, therefore, conclude that the correct assignments are as shown in Table I.

E. INDO[10] energy minimizations which constrained the species to a planar geometry with D_{6h} symmetry for the ring were performed. The resulting geometries, energies, and hfsc's are collected in Table II. These minimizations resulted in calculation of a π ground state of $^2B_1$ symmetry (C_{2v}) in each case. The minimizations were repeated for the $^2A_2$ π states in each case and additionally for the lowest σ state of the tetrafluoro- and pentafluoropyridine anions.

IV. Discussion

The absolute values of the hfs calculated by INDO for the $^2B_1$ π state of pyridine anion agree remarkably well with experiment. This also accords with the qualitative expectation

Table I. Hyperfine Splitting Constant and g Values of Fluorinated Pyridine Anions

Radical precursor	Temp, K	Isotropic hfsc's,[a,b,c] G 1	2	3	4	5	6	g value	Ref
Pyridine	198	6.82	3.55	0.82	9.70	0.82	3.55		9
2-Fluoropyridine		4.82	7.12	1.07	8.31	3.67	4.62		8
	183	5.00	6.90	1.08	8.44	3.77	4.60	2.0032	*d*
2,6-Difluoropyridine	188	4.20	0	0	10.20	0	0	2.0046	*d*
2,3,4,6-Tetrafluoropyridine	215	6.05	59.4	6.05	226	0	24.9	2.0061	*d*
Pentafluoropyridine	236	3.55	61.2	17.4	249	17.4	61.2	2.0062	*d*

[a]Underlined hfsc's belong to fluorine. [b]Accuracy of hfs and g values are ±1% and ±0.0003, respectively. [c]Zero hfsc's mean they are less than line width (see text). [d]This work.

Table II. INDO Results for Fluorinated Pyridine Anion Radicals[a]

Radical anion	State[b]		Isotropic hfsc's, G[c] 1	2	3	4	5	6	E, kcal	Geometry, Å C–C	C–F	C–H
Pyridine	$^2B_1$	π	9.00	−4.85	0.80	−8.41	0.80	−4.84	−30 746.15	1.382		1.127
	$^2A_2$	π	−3.60	−8.48	−5.89	1.03	−5.88	−8.48	−30 721.01	1.383		1.127
2-Fluoro	$^2B_1$	π	8.42	−10.0	−0.086	−8.85	1.80	−6.50	−46 874.87	1.381	1.361	1.126
	$^2A_2$	π	−3.98	8.97	−4.48	0.43	−6.42	−7.18	−46 848.50	1.382	1.362	1.137
2,6-Difluoro	$^2B_1$	π	7.86	−6.50	1.22	−9.69	1.22	−6.50	−63 002.24	1.380	1.360	1.125
	$^2A_2$	π	−4.89	8.96	−5.07	0.11	−5.07	8.96	−62 975.75	1.382	1.361	1.124
2,3,4,6-Tetrafluoro	$^2B_1$	π	7.65	−1.84	−5.74	11.7	0.43	−8.38	−95 236.41	1.382	1.361	1.122
	$^2A_2$	π	−4.65	9.59	10.5	−4.62	−4.03	10.62	−95 211.80	1.383	1.361	1.120
	$^2A_1$	σ	41.3	1506	−17.1	130	−0.76	403	−95 187.55	1.378	1.368	1.118
Pentafluoro	$^2B_1$	π	8.0	−4.39	−3.99	14.5	−3.99	−4.40	−111 349.12	1.382	1.361	
	$^2A_2$	π	−4.48	13.5	8.97	−4.0	8.97	13.5	−111 321.71	1.383	1.361	
	$^2A_1$	σ	51.2	847	−1.88	103	−1.88	847	−111 296.88	1.380	1.368	

[a]Minimizations were done by constraining the anions to pseudo D_{6h} symmetry. [b]Symmetries of states are labeled in terms of C_{2v} for simplicity. [c]Underlined hfs belong to fluorine, column 1 belongs to nitrogen, others belong to hydrogen.

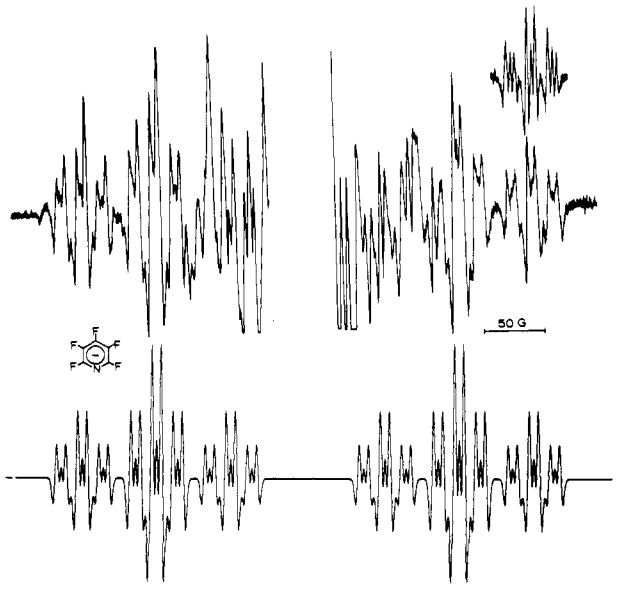

Figure 1. Second derivative EPR spectrum of pentafluoropyridine anion radical in an adamantane-Me_3NBH_3 matrix at 236 K compared with its computer simulation (below).

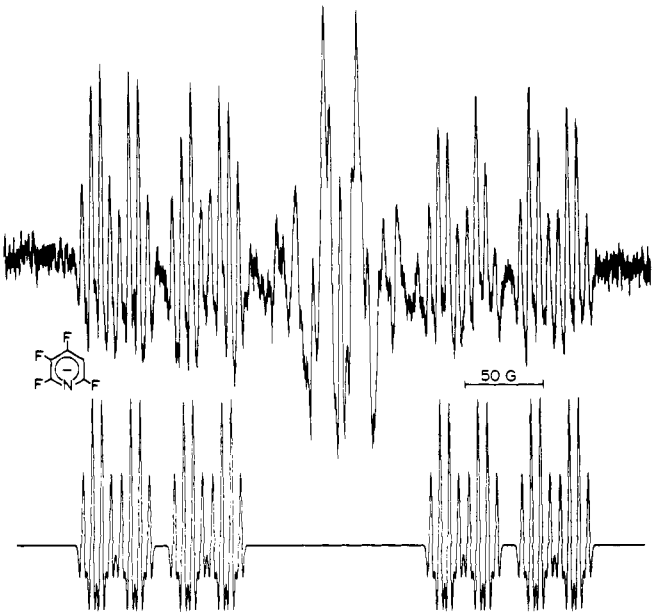

Figure 2. Second derivative EPR spectrum of 2,3,4,6-tetrafluoropyridine anion radical in an adamantane-Me_3NBH_3 matrix at 215 K with its computer simulation (below).

that the higher core potential of nitrogen will stabilize the symmetric $3b_1$ orbital and not affect the antisymmetric $2a_2$ orbital[11] (these orbitals are degenerate in benzene). The energy differences between the π states corresponding to single electron occupation of these two orbitals remain nearly constant in the fluorinated pyridine series at about 25 kcal/mol according to our INDO calculations. The trends in the calculated hfs with a single fluorine substituted at the 2-position likewise correspond reasonably well to the experimental observations. However, the 2,6-difluoropyridine anion exhibits measurable hfs only for nitrogen and the proton at the 4-position, whereas the INDO calculations indicate reasonably large fluorine hfs for the $^2B_1$ π state and in addition vanishingly small unique proton hfs for the $^2A_1$ π state.[12] The small fluorine hfs observed may be qualitatively explained by a π-donation perturbation which destabilizes the density expected at the 2- and 6-positions of the pyridine anion in the $b_1(\pi_4^*)$ orbital (compare with inset

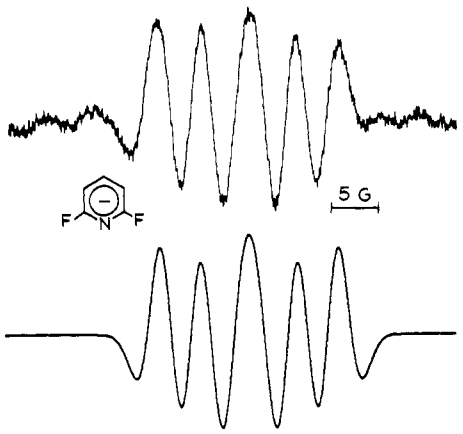

Figure 3. Second derivative EPR spectrum of 2,6-difluoropyridine anion radical in an adamantane-Me_3NBH_3 matrix at 188 K with its computer simulation (below).

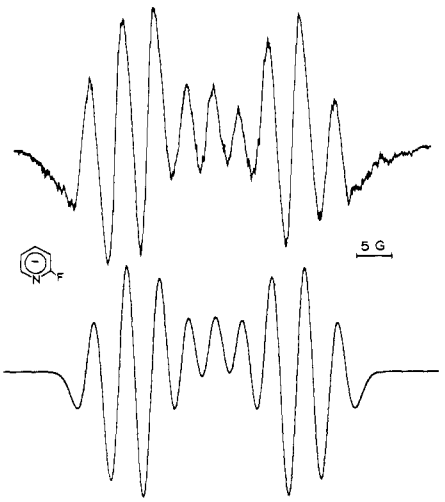

Figure 4. Second derivative EPR spectrum of 2-fluoropyridine anion radical in an adamantane-Me_3NBH_3 matrix at 183 K with its computer simulation (below).

in Figure 5). This would reduce the spin density at the 2- and 6-positions and could fortuitously cause the fluorine hfs to be nearly zero. The quantitative inaccuracy of the INDO calculation may partly arise from the D_{6h} geometry used, which requires longer CN bond distances than normal for pyridine.

Substitution of four or five fluorine atoms for hydrogen in the pyridine anion results in the same σ^*-π^* crossover phenomenon observed for the benzene anion[2] as is indicated by the tremendous increase observed for the fluorine hfs. The qualitative explanation for this phenomenon has been discussed[3] in terms of *combined effects of inductive stabilization of the σ^* orbitals and destabilization of the π^* orbitals by back donation from fluorine.* Figure 5 shows an approximate energy-level diagram of some of the highest occupied and the lowest unoccupied energy levels to summarize the σ^*-π^* orbital crossover scheme. The sequence of occupied energy levels is assigned on the basis of photoelectronic spectroscopy[13] and the unoccupied levels are assigned on the basis of our EPR results and electron transmission spectroscopy.[14] The ordering of the $b_1(\pi_4^*)$ and $a_2(\pi_5^*)$ orbitals of 2,3,4,6-tetra- and pentafluoropyridine radical anions can not be assigned by the EPR results alone; however, on the basis of the INDO calculations b_1 should be lower than a_2.

The very small hfsc's of nitrogen in penta- and 2,3,4,6-tetrafluoropyridine anions indicate that the unpaired electron

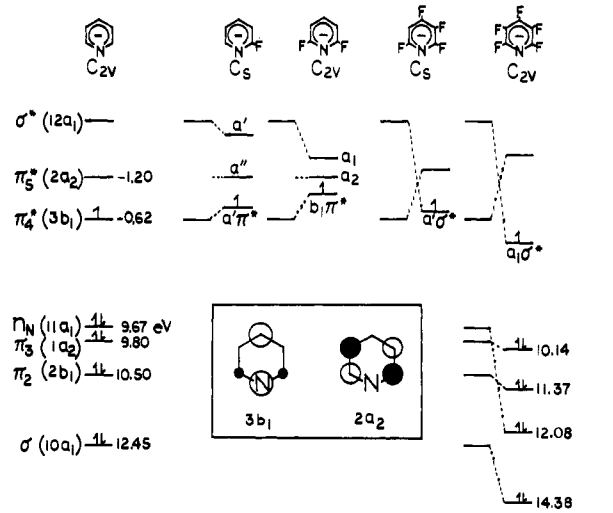

Figure 5. Approximate energy level diagram showing the σ^*-π^* orbital crossover in the fluorinated pyridine anion radicals. The energies in electron volts are from the ref 13 and 14.

σ^* orbitals have a negligible contribution from nitrogen. The large ^{14}N hfsc's calculated by INDO as well as the large value for the ^{19}F hfs at the 2- and 6-positions may arise from the distorted geometry around the nitrogen as noted above. It is clear from the numbers of equivalent ^{19}F hfs that the large hfs belongs to the fluorine at the 4-position in the case of pentafluoropyridine anion, and by analogy the large ^{19}F hfs in the case of 2,3,4,6-tetrafluoropyridine anion should also belong to the fluorine in the 4-position.

V. Conclusion

The previously unexpected phenomenon of σ anion radicals of multiply fluorinated aromatic compounds is now established. Thus, not only is the orbital pairing property of aromatic ions found to be destroyed by fluorine substitution, but also the π electron description is found to be inadequate for many cases. The availability of low-lying σ^* states should be looked into in order to explain the chemistry of polyfluoroaromatic molecules, particularly with respect to their reactions with nucleophiles. Although the stability and existence of these σ anion radicals have been demonstrated in a nonpolar matrix, it remains to be determined if they can be formed in other media.

Recently Shiotani and Williams reported the successful observation of perfluorocyclobutane anion[15] and perfluorocyclopentane anion[16] and concluded that they are σ radicals. Their results are in agreement with our conclusion of low-lying σ^* orbitals in heavily fluorinated compounds.

Acknowledgment. We acknowledge the donors of the Petroleum Research Fund, administered by the American Chemical Society, for support of this research, and the Mond Division, Imperial Chemical Industries, Ltd., for a gift of 2,3,4,6-tetrafluoropyridine.

References and Notes

(1) A. Hudson and K. D. J. Root, *Adv. Magn. Reson.*, **5**, 1 (1971), and references cited therein.
(2) M. B. Yim and D. E. Wood, *J. Am. Chem. Soc.*, **97**, 1004 (1975).
(3) M. B. Yim and D. E. Wood, *J. Am. Chem. Soc.*, **98**, 2053 (1976). The fourth line of the second paragraph on the page 2057 should be corrected to "In (S) and (A) orbitals, respectively."
(4) M. B. Yim and D. E. Wood, *J. Am. Chem. Soc.*, **98**, 3457 (1976).
(5) K. S. Chen, P. J. Krusic, P. Meakin, and J. K. Kochi, *J. Phys. Chem.*, **78**, 2041 (1974).
(6) P. J. Krusic and P. Meakin, *J. Am. Chem. Soc.*, **98**, 228 (1976).
(7) T. A. Claxton, S. A. Fieldhouse, R. E. Overill, and M. C. R. Symons, *Mol. Phys.*, **29**, 1453 (1975).
(8) A. R. Buick, T. J. Kemp, G. Y. Neal, and T. J. Stone, *J. Chem. Soc. A*, 666 (1969).
(9) G. L. Talcott and R. J. Myers, *Mol. Phys.*, **12**, 549 (1967).

(10) J. A. Pople, D. L. Beveridge, and P. A. Dobosh, *J. Am. Chem. Soc.*, **90**, 7142 (1968); J. A. Pople and D. L. Beveridge, "Approximate Molecular Orbital Theory", McGraw-Hill, New York, N.Y., 1970.
(11) A. T. Casey, R. A. Craig, and M. J. Scarlett, *J. Chem. Soc., Faraday Trans. 2*, **69**, 132 (1973).
(12) We used the representations of C_{2v} to maintain the flow of discussion for the radical anions. See Figure 5 for corresponding representations.
(13) C. R. Brundle, M. B. Robin, and N. A. Kuebler, *J. Am. Chem. Soc.*, **94**, 1466, 1451 (1972); M. B. Robin, "Higher States of Polyatomic Molecules," Vol. II, Academic Press, New York, N.Y., 1975, and references cited therein.
(14) I. Nenner and G. J. Schulz, *J. Chem. Phys.*, **62**, 1747 (1975).
(15) M. Shiotani and F. Williams, *J. Am. Chem. Soc.*, **98**, 4006 (1976).
(16) M. Shiotani and F. Williams, private communication.

Excited Potential Energy Hypersurfaces for H_4. 2. "Triply Right" (C_{2v}) Tetrahedral Geometries. A Possible Relation to Photochemical "Cross-Bonding" Processes

Wolfgang Gerhartz,[1a,b] Ronald D. Poshusta,*[1c] and Josef Michl*[1b]

Contribution from the Department of Chemistry, University of Utah, Salt Lake City, Utah 84112, and the Chemical Physics Program, Washington State University, Pullman, Washington 99163. *Received November 3, 1976*

Abstract: Ab initio VB calculations, complete within minimum basis set (STO-4G), were performed on the Born–Oppenheimer potential surfaces of the four lowest singlet electronic states of the H_4 molecule for the three-dimensional subspace of "triply right" (C_{2v}) tetrahedra. Perspective drawings of equipotential surfaces aid the visualization of the results, which include some multidimensional funnels. The results suggest a path for the known efficient quenching of $H_2(B^1\Sigma_u^+)$ by $H_2(X^1\Sigma_g^+)$ and propensity for diagonal bonding in the lowest excited singlet state in $4N$-pericyclic arrays in general, and this may be of importance for some organic photochemical mechanisms.

A previous paper in this series,[2] hereafter called part I, presented results for potential energy hypersurfaces of H_4 in the three-dimensional subspace of all trapezoids, and discussed their relation to 2s + 2s photochemical processes. In the present paper we describe results for the four lowest singlet states in a three-dimensional subspace of all "triply right" C_{2v} tetrahedra (defined below) and discuss their implications for the presently poorly understood molecular photochemistry of H_2 and for the understanding of "cross-bonding" in photochemical reactions in general.

Method of Calculation

The MB method of calculation (minimum basis set separately optimized for each state and each geometry, full configuration interaction) and the manner of presenting the results are the same as in part I,[2] which also discusses the accuracy and limitations inherent in the approach.

The geometries of H_4 presently considered are defined in Figure 1. The nuclei are labeled A, B, C, and D. The distance between A and B is denoted by $R_1 = \overline{AB}$, that between C and D by $R_2 = \overline{CD}$, and the distance between the midpoints of the lines AB and CD is labeled R. The axis connecting these midpoints is referred to as z and is perpendicular to both AB and CD, $\theta_1 = \theta_2 = 90°$. The dihedral angle, α, defined by the plane containing AB and z and that containing CD and z, is 90°. In this sense, then, the tetrahedra, ABCD, are triply right. in general, they belong to the C_{2v} point group. If $R_1 = R_2$, $R \neq 0$ and $R \neq R_1/\sqrt{2}$ the symmetry group is D_{2d}; if $R_1 \neq R_2$ and $R = 0$, the symmetry is D_{2h}; if $R_1 = R_2$ and $R = 0$, the symmetry is D_{4h}, and if $R_1 = R_2$, $R = R_1/\sqrt{2}$, the symmetry is T_d. Since the square (D_{4h}) geometries are special instances of trapezoidal geometries, they were already considered in part I, and provide an interface between the two sets of results.

When $R_1 \neq R_2$, the nuclei A and B are not equivalent to nuclei C and D. Therefore, their respective orbital exponents are not required by symmetry to be equal and were allowed to optimize to different values. Even when $R_1 = R_2$ (D_{2d}, D_{4h}, and T_d) at which all nuclei are equivalent, lower energies are frequently obtained by allowing "symmetry breaking" in the wave function, i.e., permitting the exponents of A and B orbitals to be different from those of C and D orbitals. This freedom was allowed throughout, since discontinuities in potential energy surfaces would otherwise result. The resulting wave functions do not always possess irreducible symmetry of the D_{2d}, D_{4h}, or T_d group. (See the Discussion for more detail.)

Graphical Presentation

The results to be displayed are potential energy hypersurfaces. Since four dimensions would be required to plot $E(R_1R_2R)$, we present instead a three-dimensional analogy to the well-known contour diagrams. For a given electronic state, we show a series of nested equipotential surfaces, each labeled by its energy in atomic units (Figures 2–5). The energy values at specific geometries cannot be read with great accuracy from the figures. But, then, there would be little point in a very accurate display of rather approximate results, except as a benchmark for future comparison with more accurate results, which will probably be done at selected points only. The surfaces are only approximate because of the limited nature of the basis set discussed in part I,[2] and because the grid used for their construction was relatively sparse, particularly in regions which appeared to be smooth or of little interest, in line with the general philosophy adopted (about 300 points for each state). The main purpose is to display low-energy reaction paths, minima, barriers, and avoided crossings and we believe that all such features shown in Figures 2–5 are semiquantitatively reliable. Details of slopes and absolute energy differences between surfaces of differing degrees of ionicity are not reliable, particularly those of the excited singlets.

The coordinate system for plotting the isoenergetic surfaces as a function of R_1, R_2, and R is the same as in Figure 7 of part